CHIRPED PULSE GENERATION BY CHG-FEL

H. Zen*, M. Adachi, M. Katoh, UVSOR, Okazaki, Aichi, Japan
T. Tanikawa**, SOKENDAI, Osaka, Japan
N. Yamamoto, M. Hosaka, Nagoya University, Nagoya, Aichi, Japan

Abstract

A method to generate intense and short pulse radiation from electron bunches circulating in a storage ring has been proposed. In the method, chirped pulse is generated from the electron bunches by CHG-FEL driven by chirped external laser. Overview of the method and present status of preparation for the proof-of-principle experiments are described.

INTRODUCTION

On one hand, synchrotron radiation from relativistic electron beam circulating in a storage ring has been used as X-ray, EUV and VUV sources for various spectroscopies. On the other hand, femto-second lasers recently play important role in physical researches as a source of time-resolved spectroscopy. Researches and developments aiming at generation of short pulse radiation from relativistic electron beam circulating in a storage ring have been performed so far. There are three methods; one is bunch slicing [1], another is bunch rotation [2] and the other is Coherent Harmonic Generation Free Electron Laser (CHG-FEL) [3]. By using those methods, short pulse radiations (~ 100 fs) can be generated. However those methods select or cut-out very small part of electron bunch, which usually has the bunch length of longer than 10 ps. Therefore, pulse energy of short pulse radiation is inversely proportional to the pulse duration.

To overcome above trade-off relation ship, we proposed a method which is chirped pulse generation by CHG-FEL. Chirped long pulse radiations are generated by CHG-FEL driven by chirped external laser and are compressed afterward. Proof-of-principle experiments at DUV-region are now being planned.

In this paper, overview of chirped pulse generation by CHG-FEL and present status of preparation for the proof-of-principle experiments are described.

CHG-FEL

Figure 1 shows a schematic drawing of CHG-FEL. A drive laser and an electron bunch are coaxially injected to the optical klystron. Through the FEL interaction between the laser and the electron bunch in the modulator, the energy distribution of electron bunch is sinusoidally modulated with the period length of drive laser wavelength. At the buncher section, the energy modulation is converted to density modulation due to pass length difference depending on electron energy. The electron bunch having density modulation generates harmonic radiations of the drive laser at radiator.

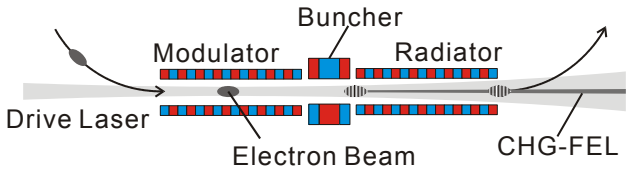

Figure 1: Schematic layout of CHG-FEL

CHIRPED CHG-FEL

A numerical code to evaluate effects of chirped driver laser has been developed [4]. A result of the code is shown in Fig. 2. The parameters of calculation are listed in Table 1. The results show that the CHG-FEL output should be linearly chirped when the driver laser is linearly chirped. Figure 3 shows the wavelength spectrum of those pulses, which obtained by the numerical code. As shown in the figure, spectral distribution is not affected by chirping of the driving laser. And radiation power of chirped case is 10 times larger than transform limited one.

From above results, we proposed a method which is chirped pulse generation of CHG-FEL. Chirped long pulse radiations are generated by CHG-FEL driven by chirped external laser and are compressed afterward.

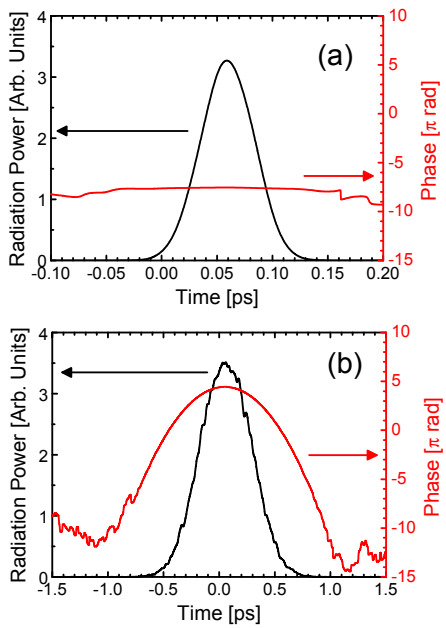

Figure 2: Temporal profile and phase shift of CHG-FEL output in 3rd harmonics of Ti:Sapphire laser obtained by the numerical simulation. (a) Result of CHG-FEL driven by transform limited pulse. (b) Result of CHG-FEL driven by chirped pulse. The phase is calculated at the wavelength of 266 nm.

*zen@iae.kyoto-u.ac.jp
Present affiliation: IAE, Kyoto Univ. Gokasho, Uji, Kyoto, Japan
** Present affiliation: PhLAM/CERLA, Villeneuve d'Ascq, France

ISBN 978-3-95450-117-5

Table 1: Parameters of numerical calculation

Electron Beam	
Beam Energy	600 MeV
Energy Spread (RMS)	3.4×10^{-4}
Optical Klystron	
Number of Periods N	9 (modulator) 9 (radiator)
Number of Equivalent Periods in Dispersive Section N_d	45
K value	6.18
Drive Laser	
Central Wavelength	800 nm
Spectrum Width (FWHM)	11 nm
Pulse Duration (FWHM)	Transform Limit (87 fs), Chirped 870 fs
Transverse Beam Size (FWHM)	5 mm
Peak Power	100 MW

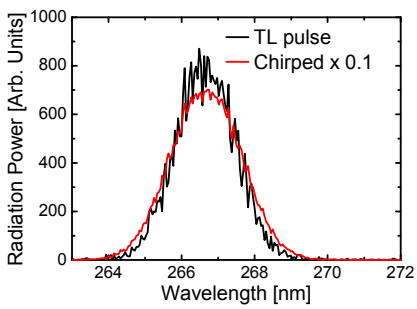

Figure 3: Wavelength spectrum of CHG-FEL at 3rd harmonics of Ti:Sapphire laser driven by transform limited pulse and chirped pulse. The transform limited pulse has 88 fs pulse duration and chirped pulse has 880 fs pulse duration and same spectral property with transform limited pulse. The radiation power of each trace is normalized by pulse duration of drive laser.

PROOF-OF-PRINCIPLE EXPERIMENT

Figure 4 shows the schematic layout of the proof-of-principle experiments, which will be performed at UVSOR-II [5]. In UVSOR-II, CHG-FEL has been intensively developed [6, 7, 8, 9, 10] and up to 9th harmonics has been observed [9]. A Ti:Sapphire laser system [11] with the maximum pulse energy of 50 mJ and the shortest pulse duration of 140 fs will be used as the drive laser of CHG-FEL. Pulse stretcher is used to give linear chirp to the drive laser. The drive laser is injected to an optical klystron installed in UVSOR-II storage ring. Then chirped CHG-FEL will be generated. The 3rd harmonic component of the CHG-FEL will be compressed at the pulse compressor. The pulse length before and after compressor will be measured by cross-correlation between fundamental laser and 3rd harmonic CHG-FEL.

Details of the pulse compressor and pulse length measurement system are shown in following subsections.

Pulse Compressor

Pulse compressor for DUV-region (266 nm) is not commercially available. Therefore we should design and construct the compressor for the proof-of-principle experiments. Figure 5 shows a schematic image of a pulse compressor using two reflective gratings, which we will construct.

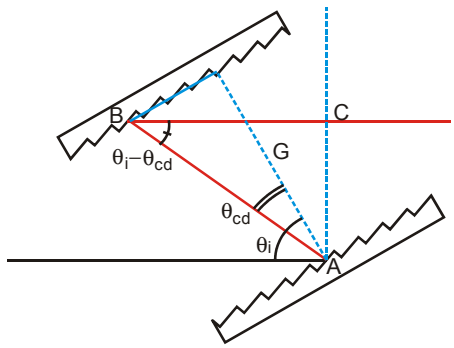

Figure 5: Schematic image of a pulse compressor using two reflective gratings.

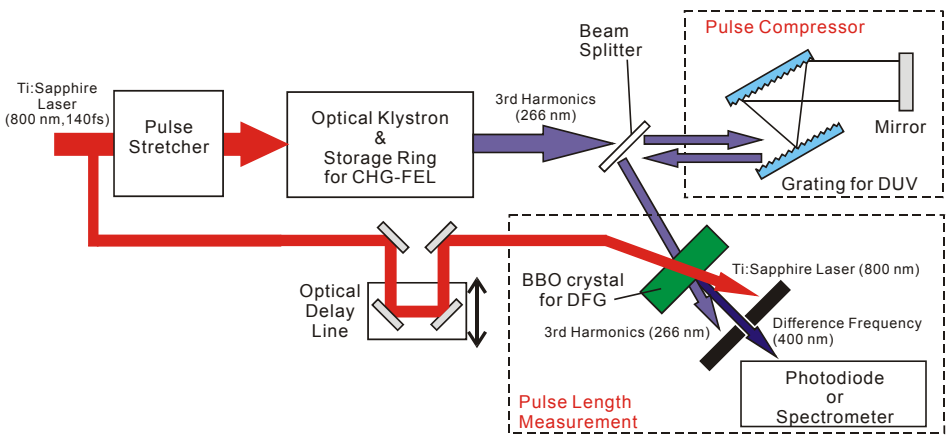

Figure 4: Schematic layout of proof-of-principle experiments.

ISBN 978-3-95450-117-5

The incident angle and blaze angle of the gratings should be carefully selected to have high diffraction efficiency. For blazed plane grating, the highest diffraction efficiency is achieved when the grating is used with blaze Littrow condition (Fig. 6). However, as shown in Fig. 5, the incident and diffracted light path are not same in case of pulse compressor. Therefore the blaze Littrow condition is not available for the pulse compressor. Second best condition for obtaining high diffraction efficiency is blaze condition. When the blaze condition is satisfied, the incident and diffracted light follow the law of reflection when viewed from the facet of grating. Usually the specification of grating in catalogues of selling companies is given as blaze wavelength at Littrow condition. To select desired grating from the catalogues, following equation is used,

$$\lambda_{B(Litt)} = \frac{2}{N}\sin\left[\frac{1}{2}\left\{\sin^{-1}(Nm\lambda_B - \sin\theta_i)\right\} + \theta_i\right] \quad (1),$$

where $\lambda_{B(Litt)}$ is the blaze wavelength at Littrow condition, λ_B is blaze wavelength in the case of incident angle θ_i, N is number of groove per unit length of grating and m is the order of diffraction. In our case, wavelength of incident light is fixed at 266 nm and we select m = 1. Then $\lambda_{B(Litt)}$ and θ_i have relationship shown in Fig. 7. For example, if we selected a grating of N = 2400 g/mm and $\lambda_{B(Litt)}$ = 300 nm, the incident angle for achieving blaze condition at 266 nm light is determined as 49 degree. And then the diffraction angle θ_{cd} is simultaneously determined as -6.7 degree from diffraction equation,

$$\sin\theta_i + \sin\theta_{cd} = Nm\lambda \quad (2).$$

From above equations, we can select a grating from catalogues and determine optimal incident angle and resulting diffracted angle.

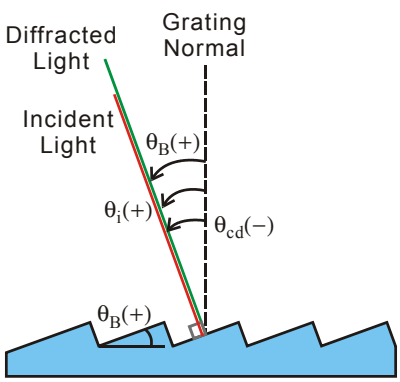

Figure 6: Blaze Littrow condition of a blazed grating.

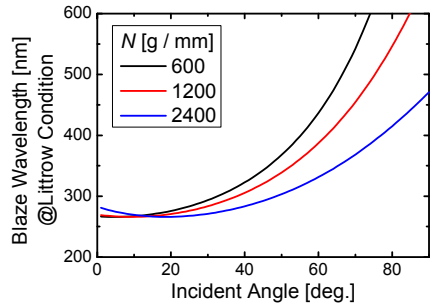

Figure 7: Dependence of blaze wavelength at Littrow condition on incident angle.

Next, we should determine the distance between two gratings in the pulse compressor. The wavelength-dependent optical path length $L(\lambda)$ in the pulse compressor (path length of A-B-C in Fig. 5) is given as

$$L(\lambda) = \frac{G}{\cos\theta_{cd}(\lambda)}\left[1 + \cos\left(\theta_i - \theta_{cd}(\lambda)\right)\right] \quad (3),$$

where G is the distance between two gratings and $\theta_{cd}(\lambda)$ is diffraction angle which depends on the wavelength of incident light. Normally, the pulse compressor is used in double pass. Therefore, optical pass will be double. As shown in Fig. 3, the expected shortest and longest wavelength of CHG-FEL in UVSOR-II is about 264 and 269 nm, respectively. The time difference between the shortest and longest wavelength is shown in Fig. 8, when those light twice pass through the pulse compressor with G = 1 m. As shown in Fig. 8, usage of gratings with large number of groove per unit length leads to large time difference, i.e. strong compression. For compressing several tens pico-second radiation in the proof-of-principle experiment, we selected N = 2400 g/mm grating for the pulse compressor. The gratings with $\lambda_{B(Litt)}$ = 300 nm and N = 2400 g/mm are commercially available. As aforementioned, when $\lambda_{B(Litt)}$ and N are fixed as those values, incident angle and diffraction angle are simultaneously determined as 49 degree and -6.7 degree if the grating is used at the blaze condition. Figure 9 shows the drawing of practical layout of the designed pulse compressor in case of 10 ps pulse compression.

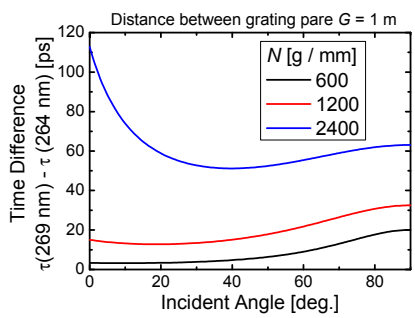

Figure 8: Time difference of 269 and 264 nm light depends on incident angle to the first grating when those light twice pass through a pulse compressor with G = 1 m.

ISBN 978-3-95450-117-5

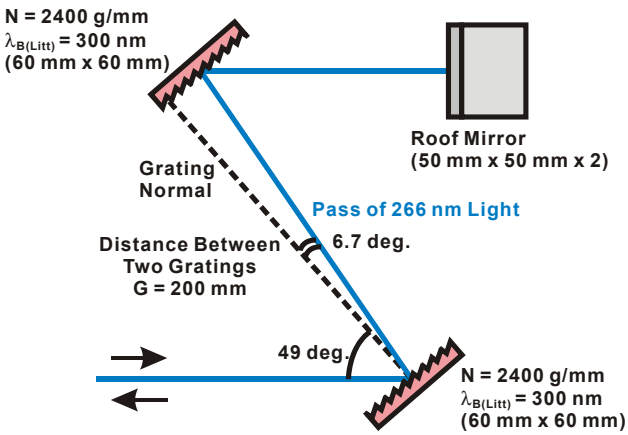

Figure 9: Layout of designed pulse compressor. The distance between two gratings is adjusted as 200 mm for 10-ps compression.

Pulse Length Measurement

The pulse length must be measured to prove the principle of proposed method at the entrance and exit of pulse compressor. For that purpose, difference frequency generation (DFG) will be adopted for cross-correlation between 266-nm and 800-nm pulses. It was reported that the pulse duration of 266 nm pulse was measured by the DFG-cross-correlation technique [12]. Same technique will be employed in our experiments.

Adjustment and Evaluation of Components

In our plan, key components such as pulse compressor and cross-correlator will be developed by us. It is quite important to adjust and evaluate those components without using electron beam, because of limited machine time of UVSOR-II storage ring. We are now planning to use a third harmonic generator (THG) based on nonlinear crystals for generating 266 nm from 800 nm (Ti:Sapphire Laser). The 266-nm light will be used for adjustment and evaluation of developed components.

SUMMARY

A method to generate intense short pulse radiation from electron beam bunch a storage ring has been proposed. By chirping the drive laser pulse of CHG-FEL, chirped coherent pulses are generated from the electron bunch. Proof-of-principle experiments at the wavelength of 266 nm will be performed in UVSOR-II. For the experiments, the dedicated pulse compressor using two reflective gratings was designed. A cross-correlator using DFG will be used for measuring the pulse length before and after pulse compressor. For adjustment and evaluation of the pulse compressor and cross-correlator, 266-nm light generated from THG nonlinear crystals will be used.

ACKNOWLEDGEMENT

This work was partly supported by Grant-in-aid for Grant-in-Aid for Young Scientists (B) No.23760067.

REFERENCES

[1] A.A.Zholents et al., Phys. Rev. Lett. **76** (1996) 912.
[2] A.Zholents, NIM A, **425** (1999) 385.
[3] G. Vignola et al., NIM A, **239** (1985) 43.
[4] H. Zen et al., Proc. of FEL2010 (2010) 286.
[5] http://www.uvsor.ims.ac.jp/defaultE.html
[6] M. Labat et al., Eur. Phys. J. D. (2007) e2007-00177-6.
[7] M. Labat et al., Phys. Rev. Lett. 101 (2008) 164803.
[8] M. Labat et al., Phys. Rev. Lett. 102 (2009) 014801.
[9] T. Tanikawa et al., Proc. of IPAC10 (2010) 2206.
[10] T. Tanikawa et al., Appl. Phys. Express **3** (2010) 122702.
[11] M. Adachi et al., Proc. of IPAC10 (2010) 2573.
[12] L. Yan et al., Proceedings of PAC07 (2007) 1052.

ISBN 978-3-95450-117-5